Chapter 3

Insertion magnets

E. Todesco[1*] *and P. Ferracin*[1]

[1]CERN, Accelerator & Technology Sector, Switzerland
[*]Corresponding author

3 Insertion magnets

3.1 Overview

The layout of the HL-LHC insertion magnets is shown in Figure 3-1 and compared to those of the LHC in Figure 3-2.

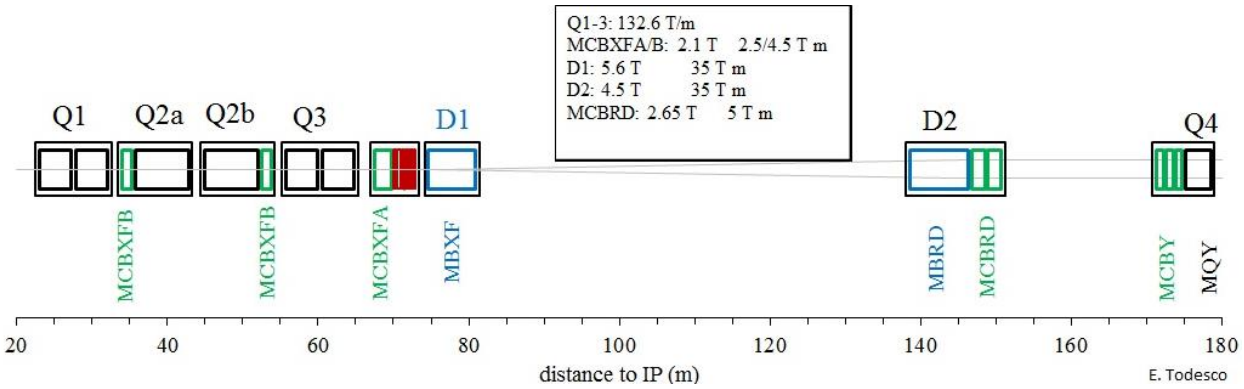

Figure 3-1: Schematic layout of the magnets in the Insertion Region (IR) region till Q4 of the HL-LHC. Thick boxes are magnets, thin boxes are cryostats.

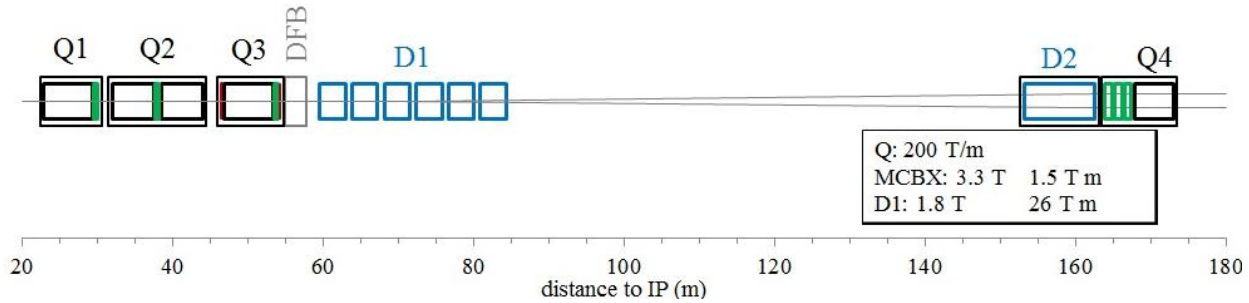

Figure 3-2**:** Schematic layout of the magnets in the current IR region till Q4 of the LHC. Thick boxes are magnets, thin boxes are cryostats.

The main technical choices can be summarized as follows [1][2]:

- Maintain the distance from the first magnet to the collision point at 23 m. This allows preserving the most critical boundaries with the detectors and the tunnel transition to the experimental cavern.

- Increase the quadrupole triplet coil aperture from 70 mm to 150 mm to allow a smaller β^* and to be able to integrate a 8/16-mm-thick tungsten (W) shielding attached to the outer surface of the beam screen; this allows reducing the effect of collision debris (heat load and radiation damage) in the magnet cold masses to the present LHC levels notwithstanding 5 times larger peak luminosity and a 10 times larger integrated luminosity.
- Select the Nb_3Sn technology for the quadrupoles [3], allowing doubling the aperture at constant integrated gradient without a too large increase in the triplet length that would make impossible the integration in the LHC tunnel. To keep the length increase below 30% while minimizing risks and costs, the following steps were taken:
    - Use in the triplet a large coil width (about 36 mm, arranged in two layers of 18-mm-wide cable) to reach maximum performance in terms of gradient [1, 4].
    - Select a working point on the loadline at 77% of short sample for nominal operation at 7 TeV [5][6][7]. This gives a 5% larger margin with respect to the LHC triplet magnets, and 9% larger margin with respect to the LHC main dipoles.
    - Fix the critical current specification to a conservative value of 1280 A/mm^2 at 15 T and 4.2 K, to avoid significant rejection of strand during production.
- Three steps are taken to recover the 10 m of additional space required by the triplet and the correctors, and to gain further space to insert the crab cavities (see Chapters 2 and 4):
    - Increase the strength of the separation/recombination dipoles from 26 T·m to 35 T·m, thus reducing the distance between the D1 and D2 centres from 90 to 75 m and recovering ~15 m.
    - Replace the 20-m-long normal conducting magnet D1 operating at 1.28 T with a superconducting 6.27 m long magnet, operating at 5.6 T [8], thus recovering ~15 m.
    - Connect the triplet busbars to the D1 through a service module on the non-IP side of D1 (not shown in Figure 3-1) instead of connecting them through a feedbox placed between D1 and the triplet as in the LHC (indicated by DFB in Figure 3-2), thus shifting the D1 towards the IP by a few metres.
- Increase the apertures of D1 and D2 dipoles and associated correctors: D1 from 60 mm to 150 mm, D2 from 80 mm to 105 mm. For the new dipoles D1 and D2, Nb-Ti superconductor has been chosen [1][2], since requirements are within reach of this technology, and the potential performance improvement given by Nb_3Sn is not sufficient to justify the additional cost and complexity. Using the LHC cable allows to reduce the risks (the cable properties are well known), to ease the schedule (lengths are already available) at the price of a larger operational current.
- Increase the strength of the three horizontal/vertical orbit correctors required in the triplet from 1.5 T·m (LHC value) to 2.5 T·m for the correctors close to Q2a/b, and to 4.5 T·m for the corrector close to Q3. The position with respect to the quadrupole magnets is the same as in the LHC layout, with the exception of the corrector between Q2a and Q2b, which is moved to between Q2b and Q3. Correctors are nested (like in the present LHC), providing both horizontal and vertical field in the same longitudinal location, to keep a compact triplet layout.
- Use a skew quadrupole to correct the triplet tilt, as in the LHC. Non-linear correctors of order 3, 4, 5, and 6 are required, both normal and skew. With respect to the LHC layout, normal and skew decapole correctors [order 5] and a skew dodecapole corrector [order 6] are added. Experience with LHC operation and field quality of the triplet short models will confirm whether these correctors are needed. In any case, the longitudinal space required for a single corrector is about 15 cm, and therefore it does not have a large impact on the layout.
- Add horizontal and vertical orbit correctors close to D2 (not present in the LHC) with a nominal strength of 5 T·m.

The main parameters of the magnets are listed in Table 3-1 and Table 3-2

Table 3-1: Overview of the main parameters of the insertion magnets – see the text for definitions of footnotes.

	Unit	MQXFA	MQXFB	MCBXFB	MCBXFA	MBXF	MBRD	MCBRD
Order		2	2	1	1	1	1	1
Aperture[1]	(mm)	150	150	150	150	150	105	105
Central field	(T)			2.10		5.58	4.50	2.59
Central gradient[a]	(T/m)	132.2						
Magnetic length[2a]	(m)	4.200	7.174	1.200	2.200	6.270	7.778	1.930
Integrated field	(T m)	556.9	948.1	2.500	4.500	35.08	35.08	5.000
Number of apertures		1	1	1	1	1	2	2
Aperture distance[2]	(mm)						188	188
Number of circuits		4 mains + 4*2		8 H + 8 V	4 H + 4 V	4	4	8 H +
Units needed (magnets)		16	8	8	4	4	4	8
Spares (magnets)		4	2	4	2	2	2	4
Cable								
Material		Nb_3Sn		Nb-Ti		Nb-Ti	Nb-Ti	Nb-Ti
Strand diameter	(mm)	0.850		0.480		0.825	0.825	0.825
Cu/No_Cu		1.20		1.75		1.95	1.95	1.30
N. strands		40		18		36	36	
Cable thickness inner[3]	(mm)	1.530		0.819		1.362	1.362	
Cable thickness outer[3]	(mm)	1.658		0.871		1.598	1.598	
Cable width[3]	(mm)	18.363		4.37		15.10	15.10	
Ins. thickness radial[4]	(mm)	0.145		0.105		0.155	0.100	0.085
Ins. thickness	(mm)	0.145		0.105		0.135	0.100	0.085
Filling factor[5]		0.294		0.229		0.243	0.253	0.132
Coil								
Number of layers		2		2		1	1	
Number of turns/pole		50		140 / 191		44	31	3650
Cable length/pole		431	721	390 / 515	670 / 900	556	530	2200
Operational parameters								
Peak field[6]	(T)	11.41		4.13		6.58	5.26	2.94
Temperature	(K)	1.9		1.9		1.9	1.9	1.9
Current[a]	(kA)	16.23		1.625/1.474	1.584/1.402	12.11	12.33	0.394
Overall current	(A/mm^2)	469		314 / 285	306 / 271	449	478	702
Loadline fraction[8]		0.77		0.51	0.50	0.77	0.68	0.47
Temperature margin	(K)	5.0		4.1	4.1	2.4	3.0	4.2
Stored energy/m	(MJ/m)	1.17		0.064/0.119	0.061/0.109	0.340	0.291	0.074
Inductance/m	(mH/m)	8.21		48.7 / 105		3.97	3.52	480
Stored energy[9]	(MJ)	4.91	8.37	0.077/0.143	0.134/0.239	2.13	2.26	0.143
Mechanical structure								
Forces x	(MN/m)	2.47		0.322		1.52	0.67	
Forces y	(MN/m)	-3.48		0.402		-0.65	-0.57	
Midplane stress[10]	(MPa)	108		25		91	51	
Protection								
Circuit inductance[11]	(mH)	255		58.4 /124.8	107.1/232.3	24.9	27.4	920
Coil energy density[12]	(J/mm^3)	0.078		0.027	0.025	0.071	0.045	0.122
Dump resistor	(mΩ)			0.15	0.15			1.4
Heater circuits[13]		8	8			4	8	

[1]Aperture is the coil inner diameter at room temperature, excluding ground insulation, cold bore, and beam screen.
[2]Distance between apertures and magnetic length are given at 1.9 K.
[3]Strand/cable dimensions are given at room temperature, in the case of Nb_3Sn after reaction.
[4]Insulation dimensions are given at room temperature.

[5]Filling factor is defined as the fraction of superconductor in the insulated cable.
[6]Peak field in the coil is given including the contribution of the strand where the peak is located (self-field correction).
[7]Overall current density is the average over the whole cross-section of the insulated cable (i.e. including voids or impregnation and insulation, but not copper wedges); for the MCBRD overall current density is referred to the cross-sectional area of the slot.
[8]Load line fraction is the ratio between the operational current and the critical current on the load line.
[9]Stored energy is given for the whole magnet: in the case of independently powered apertures or nested magnets, stored energy is given for both circuits powered with maximum nominal current.
[10]Midplane stress is an estimate given by the accumulation of the azimuthal Lorentz forces at nominal current divided by the coil radial width – the impact of the structure, preload, and bending is not considered.
[11]Circuit inductance is the differential inductance of the circuit at nominal current.
[12]Energy density is given over the coil volume, including insulation but not coil parts such as copper wedges and pole pieces.
[13]Heater circuit are the available number of heater circuits per magnet; to know how many are actually used, see Chapter 7.
[a] Values for the nominal current, gradient in the straight section and magnetic length for the Q1, Q2 and Q3 magnets based on present results.

Table 3-2**:** Overview of the main parameters of the triplet corrector magnets.

	Unit	MQSXF	MCSXF/ MCSSXF	MCOXF/ MCOSXF	MCDXF/ MCDSXF	MCTXF	MCTSXF
Order		2	3	4	5	6	6
Aperture	(mm)	150	150	150	150	150	150
Integrated strength[1]	(T m)	0.700	0.095	0.069	0.037	0.086	0.017
Coil length[2]	(mm)	456.8	191.5	171.5	171.7	498.3	123.3
Gradient	(T/m^{n-1})	34.8	224	3680	40480	585600	550400
Number of apertures		1	1	1	1	1	1
Number of circuits		1	2	2	2	1	1
Units needed		4	8	8	8	4	4
Spares		2	4	4	4	2	2
Cable data							
Material		Nb-Ti	Nb-Ti	Nb-Ti	Nb-Ti	Nb-Ti	Nb-Ti
Strand diameter	(mm)	0.700	0.500	0.500	0.500	0.500	0.500
Insulation thickness	(mm)	0.070	0.070	0.070	0.070	0.070	0.070
Cu/No_Cu		2.1	2.1	2.1	2.1	2.1	2.1
Coil design							
N. turns/pole		754	288	372	228	432	432
Cable length/pole	(m)	1230	104	105	59	439	112
Operational parameters							
Coil peak field	(T)	3.60	2.23	2.09	1.63	1.57	1.50
Temperature	(K)	1.9	1.9	1.9	1.9	1.9	1.9
Current	(A)	174	99	102	92	85	84
j overall[3]	(A/mm^2)	314	308	317	286	264	261
Loadline fraction	(a dim)	0.44	0.31	0.31	0.26	0.27	0.27
Temperature margin	(K)	4.3	4.9	4.9	5.2	5.0	5.0
Differential	(mH)	1530	213	220	120	805	177
Stored energy	(kJ)	30.8	1.72	1.55	0.668	3.627	0.732

[1]Integrated strength is defined as the field at the 50 mm reference radius times the magnetic length.
[2]Coil length refers to the physical coil length, and not to magnetic length.
[3]The overall current density includes 0.07 mm thick strand insulation and the coil ground insulation.

After TDR 0.1 [9] several design decisions were adopted:

- MQXF shimming in order to modify the systematic harmonics b6 of the MQXF quadrupole [47].
- Increase of the iron yoke hole diameter from 60 to 61 mm for heat exchangers in D1 and MCQSXF [49].

- Triplet protection: after validation on short models and prototypes, CLIQ has been selected as baseline for protection with outer layer heaters [10].
- Nested corrector protection: a 0.15 Ω dump resistor adopted for both MCBXFA and MCBXFB [10].
- Triplet circuit: the 120 A trim on Q2a has been removed, since the spread between the integrated transfer function of the quadrupoles was deemed to be well within the tolerance range, and sorting could be used as an additional way to reduce this spread.
- Triplet circuit: a 35 A trim on Q1a has been added for beam optics measurements [10].
- High order correctors: to better correct the measured triplet errors there has been one iteration on the corrector strengths, keeping the same length of the cold mass, with a 30% reduction of the skew quadrupole and by 50% increase of sextupole, octupole and decapole (normal and skew) [44].
- Q4 and Q5: both the Q4 LHC cold mass and the Q5 LHC cold masses shall be reused for the HL-LHC, with operational temperature of 4.5 K as in the LHC.
- Q5 in IR6: no modifications with respect to the LHC layout [46].
- A consolidation action of the resistive magnet has been carried out, adding shielding to reduce the radiation damage. This removes the need of construction of new resistive magnets initially foreseen [48].
- Implementation of the Fully Remote Alignment system allowing to reduce the required correctors strength [43].
- Optimization of the alignment of the D1 to maximize the beam aperture [42].

3.2 Low-β triplet quadrupoles

Function, operational modes, and powering: The triplet magnets, denoted by MQXF, ramp with the energy of the LHC, with a nominal gradient of 8.5 T/m at 450 GeV, and a maximal operational gradient of 132.2 T/m at 7 TeV. During squeeze, its gradient is constant or decreases by not more than 10%. The triplet quadrupoles, Q1-Q2a-Q2b and Q3, are powered in series, with a 2 kA powering trim acting on Q1 and another one on Q3. The quadrupoles Q1 and Q3 are produced by the USA DOE project HL-LHC AUP (see Chapter 1) and Q2a and Q2b by CERN.

Conductor: The Nb_3Sn cable has 40 strands, with 0.85 mm diameter [7]. The main specifications are:

- A minimum non-copper critical current density of 1280 A/mm^2 at 15 T and 4.2 K; this value has been lowered in 2015 with respect to the initial specification of 1400 A/mm^2 to avoid the rejection of a significant part of the production.
- The cable keystone angle has been fixed to a conservative value of 0.40° to reduce the critical current degradation of cabling below the 5% specified value; this value has been reduced from the initial 0.55° to reduce cabling degradation for PIT strand.
- RRR larger than 100 after cabling.
- Cu/no Cu ratio of 1.2 (54.5% of copper in the strand) to have a good compromise between critical current density and protection.
- The cable has S2^{TM} glass braided insulation, whose thickness is 145 μm at 5 MPa before reaction.
- The cable contains a 12-mm-wide, 25-μm-thick stainless-steel core to control and reduce the dynamic effects.

Coil, current density, and margin: Having two coil layers, one can reach the operational gradient of 132.2 T/m at 77% of the short sample limit on the load line (i.e. 23% of load line margin). Each layer has a copper wedge to tune field quality.

Lengths and transverse size: The triplet is made of Q1 and Q3 magnets, each unit requiring a magnetic length of 8.4 m; plus Q2 with a 14.3-m-long magnetic length. In the initial phase of the project, US-AUP decided to split both Q1 and Q3 into two 4.2-m-long magnets, assembled in the same cold mass, to reduce the risks associated to manufacturing long magnets. CERN decided to split the Q2 into two 7.17-m-long magnets called Q2a and Q2b. The Q1, Q2, and Q3 cross-sections are identical, and make use of the same design, technologies, and (almost all) components. The cold mass cross-section has a 630 mm diameter, i.e. 60 mm more than the LHC dipoles including the stainless-steel vessel.

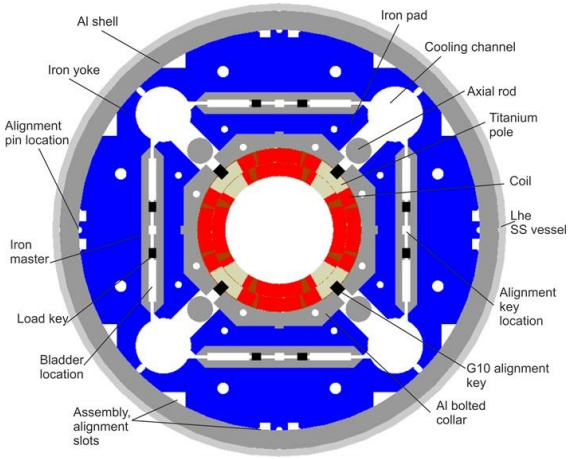

Figure 3-3: Sketch of triplet quadrupole magnet cross-section.

Mechanical structure: The quadrupole makes use of a shell-based structure developed at LBNL and within the LARP collaboration with a series of short models called TQS [11]. The structure scale-up to a length of 3.4 m, was demonstrated in the LARP LR and LQ quadrupole models [12], and features to assure alignment in operational conditions have been included in the 120 mm aperture HQ short model quadrupole [13]. The MQXF cross-section is a scale up of the HQ design. Coils are mainly pre-stressed by the Al shell during cool-down, acting as the structure to contain the Lorentz forces. The level of stress is fine-tuned during the loading of the coil, which is done at room temperature using water-pressurized bladders and interference keys. Typically, one has ~70 MPa of azimuthal coil compression at room temperature, which becomes ~150 MPa at 1.9 K thanks to the interplay of the thermal contractions of the different components. The structure keeps the coil under compression up to the ultimate current, corresponding to 143.2 T/m (7.5 TeV operation).

Protection: The energy density in the coil is ~0.08 mJ/mm^3 (with coil volume including insulation, but excluding wedges), which is ~50% larger than the LHC main magnets [14]. This makes quench protection challenging. Since the circuit inductance is of about 250 mH, only a small fraction (~5%) of the energy can be extracted on a dump resistor. Therefore, we have to rely on quench heaters on the outer layer of the coil, and no dump resistor is included in the circuit. Quench heaters are 25 µm stainless steel strips with a 50 µm polyimide layer to ensure proper insulation. The heaters will have heating stations of 40 mm length, separated by 120 mm sections with lower resistance due to a 10 µm copper cladding (see Figure 3-4). The width of the heating stations is 20 mm, and a 7.17-m-long magnet will have ~40 heating stations. Two independently powered strips will cover the two blocks of the outer layer. The typical time needed to quench the coil at nominal current is of the order of 15–20 ms following heater firing [15]. Assuming 5 ms for detection time, a validation window of 10 ms and a few ms for switch opening, this brings the hotspot temperature to ~350 K [16]. To reduce this value and to ensure some redundancy, we also use the CLIQ system [17], recently developed at CERN, based on coil heating induced by an induced oscillating current in the magnet. The CLIQ system has the interesting feature of acting rapidly on the inner layer and is therefore complementary to the outer layer quench heaters. It has been validated on all short models and on the US prototypes, allows reducing the hotspot temperature of about 70 K, i.e. from 350 K (outer layer quench heaters) to 280 K (outer layer quench heaters and CLIQ). However, CLIQ is less effective at low current and cannot protect the magnet at injection current.

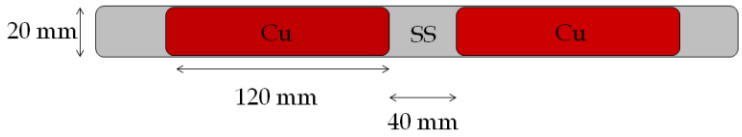

Figure 3-4: Quench heaters for the outer layer. Stainless steel (SS) in grey and copper cladding in red. A ~300 mm long portion, out of the 4/7 m long strip, is shown.

Field quality: Allowed field harmonics (b_6, b_{10}) are optimized for operation at high field, and are expected to be below one unit in absolute value. Contributions from the coil ends are also taken into account and compensated when possible through the straight part [18]. Random components are estimated for a 25 μm random error in the block positioning for non-allowed, and 100 μm for allowed; most critical components are low-order harmonics (b_3, a_3, b_4, a_4). To minimize these components we opted for a strategy similar to that used in the RHIC magnets [19], with magnetic shims to be inserted in the bladder location [20]. This allows correcting (i) ±5 units of b_3; (ii) ±5 units of a_3; (iii) ±3 units of b_4; (iv) ±1 units of a_4, for a maximum of two harmonics at the same time, through an asymmetric magnetic shimming. A fine-tuning of b_6 has been done at the beginning of the prototype phase, to increase it from -4 to 0 units through the addition of a 125 μm shim in the coil pole and a reduction of 125 μm shim in the midplane.

Cooling: The magnet is in a static bath of pressurized HeII, with a welded stainless-steel shell placed outside the Al structure acting as a helium vessel. Cooling is ensured via two heat exchangers of 68 mm inner diameter, in which a saturated HeII bath is formed, housed in the 77 mm diameter holes of the iron located in the upper part, see Figure 3-3 [21]. The heat exchanger cools the triplet and the short orbit correctors MCBXFB, with the separation dipole and corrector package on a different circuit. With this design, one can comfortably remove ~800 W of heat load from the triplet, i.e. 675 W at ultimate luminosity on the cold mass given by debris (see Table 3-1), plus a 125 W budget for other loads (among them the 25 W load of collision debris ending on interconnections), at the ultimate peak luminosity. To cope with these high heat loads, a low pressure pumping is added between Q2a and Q2b to keep the two-phase vapour flow velocity below 7 m/s, above which the Heat exchangers (HXs) would not function correctly [50].

For the Nb-Ti coils in the LHC, the peak heat deposition target was set at 4 mW/cm^3; this has a factor of 3 safety on 12 mW/cm^3, which was considered to be the hard limit. Later experience showed that the hard limit is at least a factor of two larger. In the HL-LHC, thanks to the tungsten shielding, we are always below the 4 mW/cm^3 target, as shown in Table 3-1. The Nb_3Sn superconductor in the present MQXF design is expected to have a peak power limit of the order of about 70 mW/cm^3, i.e. one order of magnitude larger than the load in the HL-LHC. The heat loads from the coils, from the cold mass and from the beam-pipe area can only be evacuated to the two heat exchangers by means of pressurized HeII. To this aim the cold mass design incorporates the required helium passages: 1.5 mm annular spacing between cold bore and inner coil-block, and free passage through the coil pole and subsequent G10 alignment key. The free passage needed through the coil pole and G10 alignment key in the transverse direction is given by 8 mm diameter holes repeated every 50 mm.

The beam screen receives ~500 W in the triplet–correctors–D1 region (including 55 W from the interconnections). Given the 100 W budget for the residual effect of electron cloud, and the 50% margin for getting to ultimate luminosity, the system has to remove ~1000 W over 55 m, i.e. ~17 W/m. Heat is removed at 60-80 K [41]. The cooling tubes inner diameter is ~7 mm, due to an increase of the pressure of the helium to 18 bar. This choice is more challenging for the piping system but allows minimization of the space taken by the cooling pipes, which reduce the aperture available to the beam.

Cryostat: Independent cryostats are used for Q1, Q2a, Q2b, and Q3. The Q1 and Q3 cryostats contain two 4.2-m-long magnets. The Q2a and Q2b cryostats contain each one 7.17-m-long magnet plus the orbit correctors described below. The cryostat size should be able to accommodate the cold mass, the thermal shielding, and the cooling pipes. The LHC standard vacuum vessel size of 980 mm (including flanges) is a tight fit for all of

these components. To solve this problem, we use asymmetric centering to make room for the piping in the upper part of the cryostat (see Figure 3-5).

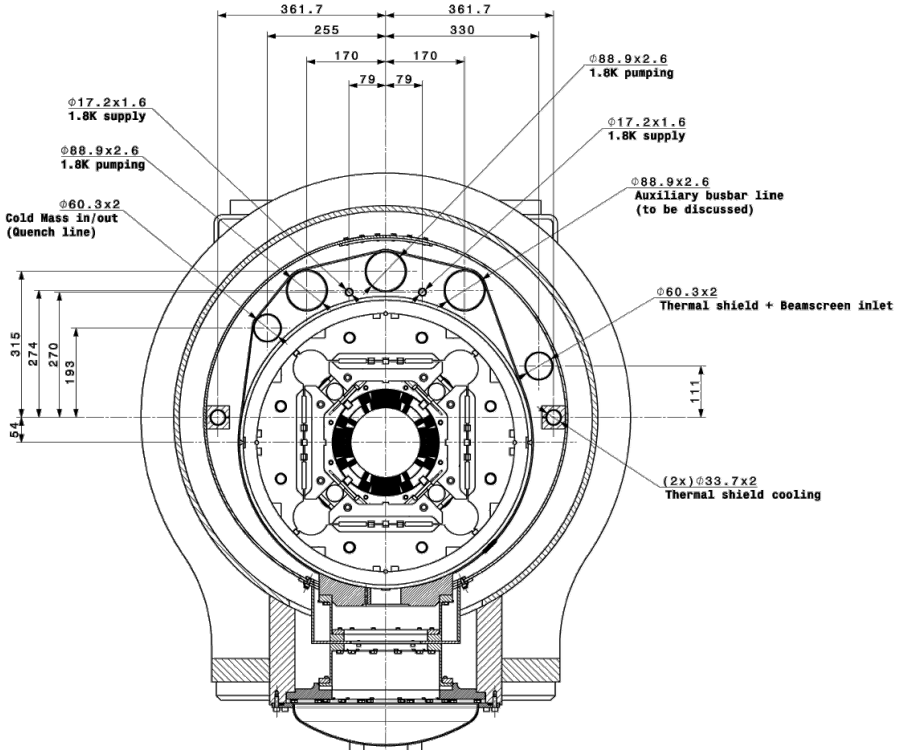

Figure 3-5: Cross-section of the cryostat.

3.3 Nested orbit correctors

Function, operational modes and powering: The orbit correctors are single-aperture magnets. Two versions are required, providing 2.5 T·m and 4.5 T·m integrated fields. To have a more compact layout in this region where longitudinal space affects performance, a nested design has been adopted, with the horizontal and vertical dipole coil in the same cross-section (see Figure 3-6). The field in each plane has been limited to 2.1 T, giving a maximum combined field of 3 T. Powering will be allowed in a square in the horizontal/vertical plane, with both positive and negative currents. These magnets generate the crossing angle and correct the quadrupole misalignment.

Orbit corrector prototypes have been developed by CIEMAT (Madrid, ES), which provides the series magnets in the framework of a collaboration agreement [23].

Conductor: The 4.5-mm-wide Nb-Ti cable developed for the SLHC corrector [24] has been adopted. This is based on a 0.48-mm-diameter strand, arranged in a Rutherford cable with 18 strands. The cable is insulated with a braided S2-glass as the MQXF.

Coil, current density and margin: The magnets have two-layer coils per dipole direction; this allows reaching the operational field of 2.1 T simultaneously in both planes at less than 50% of the load line. The coil has a large number of turns (up to 200) and it is impregnated with CTD-101K® as the MQXF to ensure a proper control of the dimension and to allow magnet assembly.

Lengths and transverse size: The magnetic length is 1.2 m for the short version (MCBXFB) and 2.2 m for the long one (MCBXFA). The magnet cross-section has a 630 mm diameter, including the stainless steel helium vessel (not shown in Figure 3-6), i.e. as in the HL-LHC triplet.

Mechanical structure: The magnet makes use of self-supporting collars. Stainless steel collars are used for keeping the inner and outer coils in place. Their thickness is 25 mm. Due to the nested coil arrangement, a

complex collaring based on two consecutive steps (first the inner, then the outer) is needed. The inner collars are closed with two round pins; the outer ones will be kept in place by four prismatic keys. A particular difficulty is that when both horizontal and vertical coils are powered, electromagnetic forces push the inner coil towards the centre of the aperture: for this reason, the preload must exceed the compression due to e.m. forces.

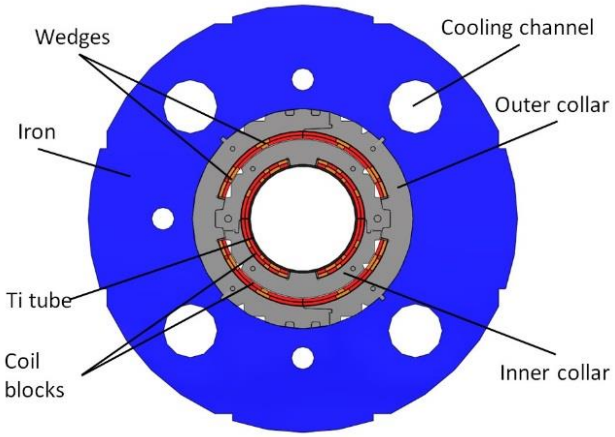

Figure 3-6: Orbit corrector cross-section (both MCBXFA and MCBXFB).

Protection: The magnets are protected via a 0.15 Ω dump resistor, keeping hotspot temperatures within 250 K.
Field quality: The magnet multipoles shall be within a window of ±20 units at maximum current in one field direction for all powering configurations of the other field direction. This is ensured by the cross-section and proper shaping of the iron.
Cooling: The MCBXFB magnet will share the same cold mass of the triplet Q2a/Q2b; cooling is ensured via the 68-mm-diameter heat exchangers placed in the 77-mm-diameter iron hole at 45º; a minimum of 1.5 mm gap between cold bore and magnet is also guaranteed for heat extraction.
The MCBXFA magnet will share the cold mass with the high order correctors; simulations show that a solution with one (or more) heat exchangers cooling the whole string triplet–corrector package-D1 is not viable. Therefore, a second system of heat exchangers is used to cool the corrector package and D1. Here the baseline is to have two heat exchangers of 49 mm inner diameter, reusing the LHC ones, able to remove 250 W. One heat exchanger would provide only 125 W.
Cryostat: The cryostat of the corrector package will have a similar design and features as the triplet cryostat, described in 3.2.

3.4 High-order correctors

Function, operational modes and powering: The high-order correctors (skew quadrupole, normal and skew sextupole, octupole, decapole, and dodecapole) are specified based on the expected field quality and alignment errors of the triplet magnets and separation-recombination dipoles (see Chapter 2), with a safety factor of 2 for the quadrupole, sextupole, and octupole, and 1.5 for the decapole and dodecapole components. The magnets will operate with nominal settings based on the measured field errors of the triplet and of the separation dipole. To ease operation, a non-nested layout (see Figure 3-7) has been adopted, using a superferric technology (see Figure 3-8 and Figure 3-9), already developed for the SLHC-PP [25]. Nb-Ti racetrack coils provide the ampere-turns, with iron giving the required field shape. The aperture is 150 mm, as for the triplet and D1.

The high-order corrector prototypes have been developed by the LASA laboratory of INFN (Milano, IT), which also provides the series magnets in the framework of a collaboration agreement.

Conductor: The cable is a single Nb-Ti strand, of 0.7-mm-diameter for the quadrupole and of 0.5 mm diameter for the higher order multipoles. Insulation is made with a 0.07-mm-thick S2 glass. Ground insulation is added on the external side of the coil.

Coil, current density, and margin: We chose to operate at 25% to 45% on the load line. The optimized current density is of the order of 300 A/mm^2 [26], with peak fields on the coil in the range of 1.5-2.3 T for the nonlinear correctors and 3.6 T for the skew quadrupole (see Table 3-2). Coils are dry-wound and then vacuum impregnated with CTD-101K®. Currents are below 120 A for all correctors to be able to reuse the LHC power converters, with the exception of the quadrupole corrector that requires 200 A.

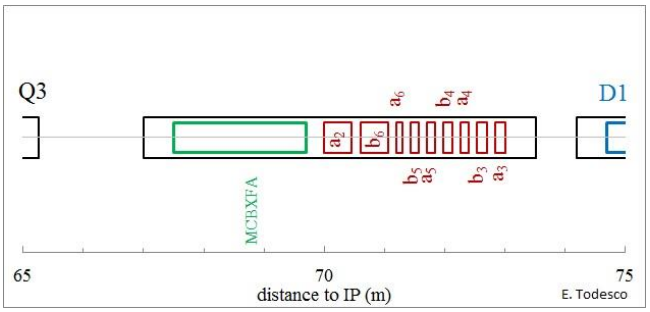

Figure 3-7**:** Layout of the corrector region.

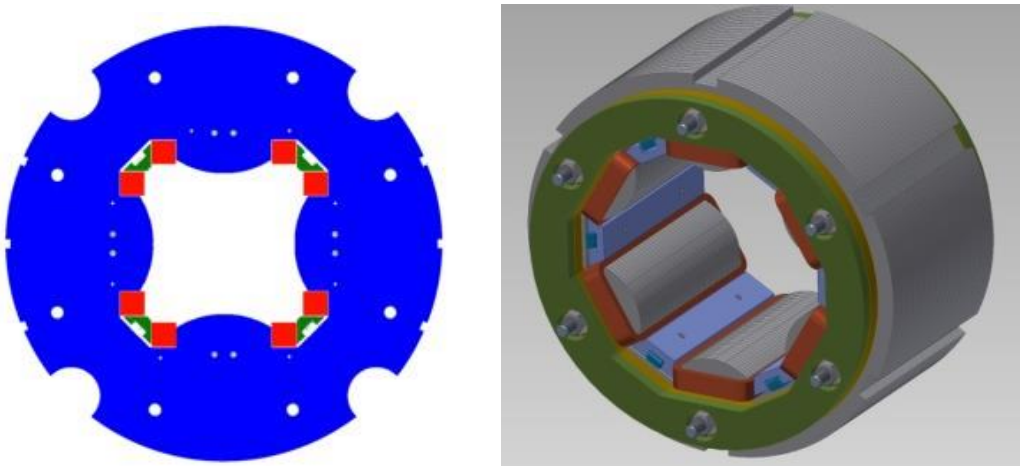

Figure 3-8**:** Cross-section of the skew quadrupole and 3D view of a sextupole (right).

Lengths and transverse size: The magnet lengths are 200 to 250 m for the sextupole, octupole, decapole, and skew dodecapole (see Table 3-2). The normal dodecapole and the skew sextupole require greater strengths, giving a magnet length of about 600 mm. The skew quadrupole needs a 460 mm diameter iron yoke that has to include indents for the cooling pipes for the heat exchanger. The nonlinear correctors can have an iron yoke diameter of 320 mm, which fits inside the cooling pipes. Spacers are required to match the transverse size of the correctors to the same value of the MCBXFA orbit correctors, and to maintain alignment within the cold mass. Heat exchangers will go through these spacers to cool the whole cold mass.

Mechanical structure: The mechanical support is guaranteed by wedges screwed to the structure (in green in the figures). The forces are of the order of 60 kN/m for the quadrupole and 10-30 kN/m for the other magnets.

Protection: The skew quadrupole protection relies on a dump resistor of 0.7 Ω; for the other magnets, the quench propagation is enough to protect the magnet with a hotspot below 200 K.
Field quality: Field quality requirement is to have all harmonics below 100 units at the reference radius of 50 mm. By design the harmonics are 10 times lower.
Cooling: Cooling of the helium bath is ensured by heat exchangers as described in 3.3. No requirement is needed on the stacking factor of the laminations. A wide gap between the Nb-Ti coils and the cold bore ensure free He passage in the inner part of the magnet.
Cryostat: As described in 3.3.

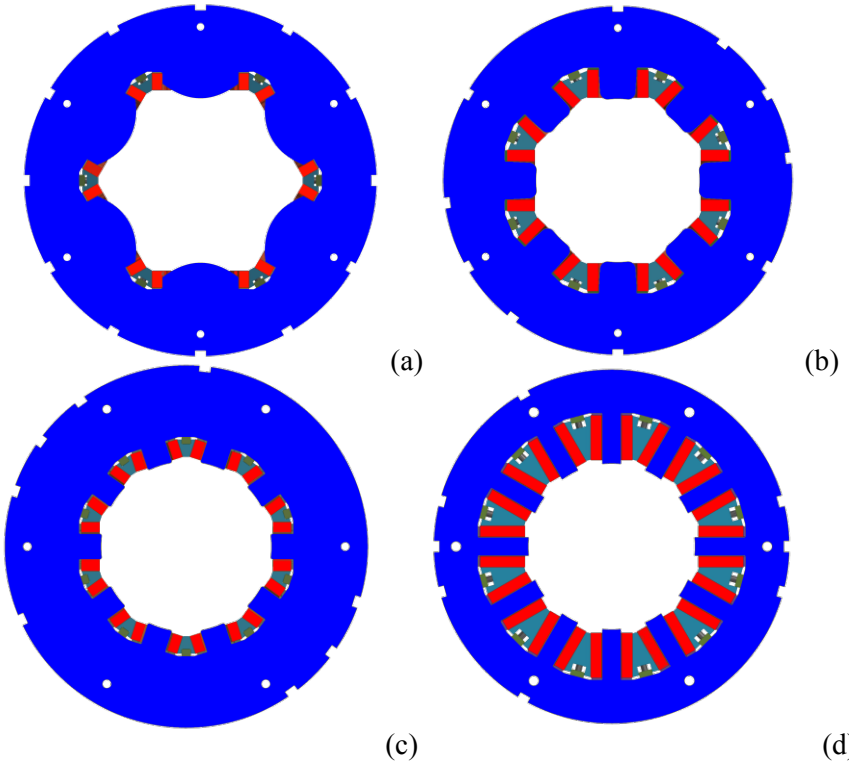

Figure 3-9: Sketch of nonlinear corrector cross-sections of (a) normal sextupole; (b) normal octupole; (c) normal decapole; (d) normal dodecapole correctors.

3.5 Separation dipole D1

Function, operational modes and powering: The separation dipole is ramped with the energy of the LHC and is constant during squeeze. D1 is individually powered.

The separation dipole short models and prototypes have been developed by KEK (Tsukuba, JP), which also provides the series magnets as in-kind contribution.

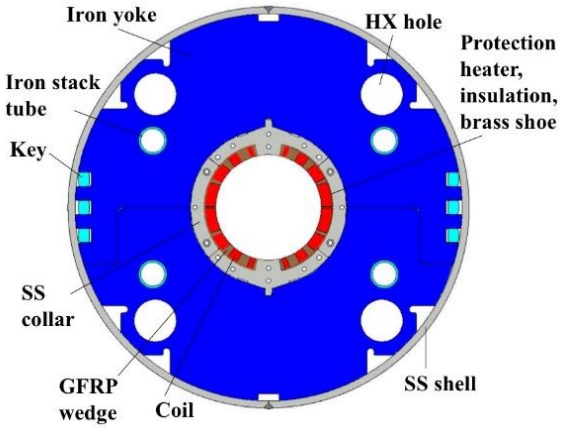

Figure 3-10: Cross-section of the MBXF magnet.

Conductor: The 15-mm-width Nb-Ti cable used for the outer layer of the main LHC dipole is adopted. The required unit length is about 2/3 of the main LHC dipole outer cable unit length (780 m).

Coil, current density and margin: With the initial choice of 70% operational level, the magnet length was slightly longer than the KEK test station [8][27]. We therefore fixed the operational current at 77% of the load

line, with a bore field of 5.6 T: this allowed fitting the vertical test station without significantly increasing the risk related to the lower margin.

Lengths and transverse size: Magnetic length is 6.27 m. The magnet cross-section has a 570 mm diameter, including the stainless-steel vessel, i.e. the same as the LHC dipoles. A larger diameter has been excluded to be able to reuse the yoking tooling used for J-PARC at KEK.

Mechanical structure: Forces are contained by the iron yoke, with thin spacers between the iron and the coil, as the J-PARC [28], RHIC magnets [29], and LHC Q1/Q3 [30]. Here the pre-stress is given by the iron laminations, horizontally split, that are locked through keys (see Figure 3-10). A thin stainless-steel collar acts as a spacer between the coil and the iron yoke. An alignment notch at 90° and 270° has been added after a first collaring test. An average pre-stress of 90 MPa is given at room temperature during the so-called 'yoking'. During cool-down the pre-stress lowers to 70 MPa, which is enough to counteract the Lorentz forces during powering.

Protection: The magnet shall be protected with quench heaters based on the same LHC technology and no energy extraction; hotspot temperature shall be within 300 K.

Field quality: The main issue here is the saturation component [8], which is optimized via the iron shaping. Following the analysis given in Refs. [31][32], the random components are estimated through random positioning of the coil block with different amplitudes for each family of harmonics, namely 40 µm for the allowed b_{2n+1}, 30 µm for the even skew a_{2n}, 15 µm for the odd skew a_{2n+1},and 10 µm for the even normal multipoles b_{2n}.

Cooling: The magnet is in a static bath of pressurized HeII, with a stainless-steel shell acting as a helium vessel. First baseline, showed in Figure 3-10, had cooling is ensured via two heat exchangers, of 49 mm inner diameter, housed in the 60 mm diameter holes through the iron. The position of the heat exchanger is the same as in the triplet to ease the interconnections.

Cryostat: The cryostat has the same geometry as the triplet cryostat (see Figure 3-5).

3.6 D1-DFX connection module (DCM)

Function: The DCM is the module that connects D1 to the distribution feedbox (DFX, see Chapter 6A), see Figure 3-11 and Figure 3-12. The module has on the one side the connection to the D1 cryostat, and on the other side the lambda plate with the transition from 1.9 K to 4.2 K. The module contains the five busbars of the 18 kA circuit, including trims, the two busbars of the 13 kA circuit of the D1, and the six busbars of the nested correctors MCBXFA/B. These busbars go through the lambda plate, where they are joint to the Nb-Ti busbars of the cold powering(see Figure 3-11). After the insertion of the "cold" diodes in the triplet circuit, this module has also the function of housing the stack of four diodes in a chimney whose position is optimized to minimize the radiation dose.

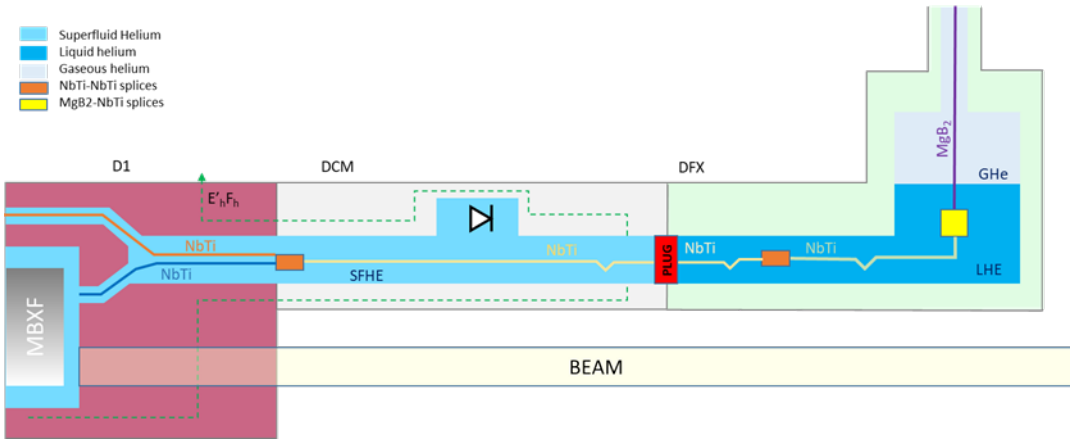

Figure 3-11: Conceptual design of the D1-DFX connection module

Conductor: All busbars are based on the same round cable using Nb-Ti strands used in WP6a (see Chapter 6A).

Lengths and transverse size: The module is 8 m long, thus requiring an adequate mechanical support and careful treatment of the fixed points and thermal contractions.

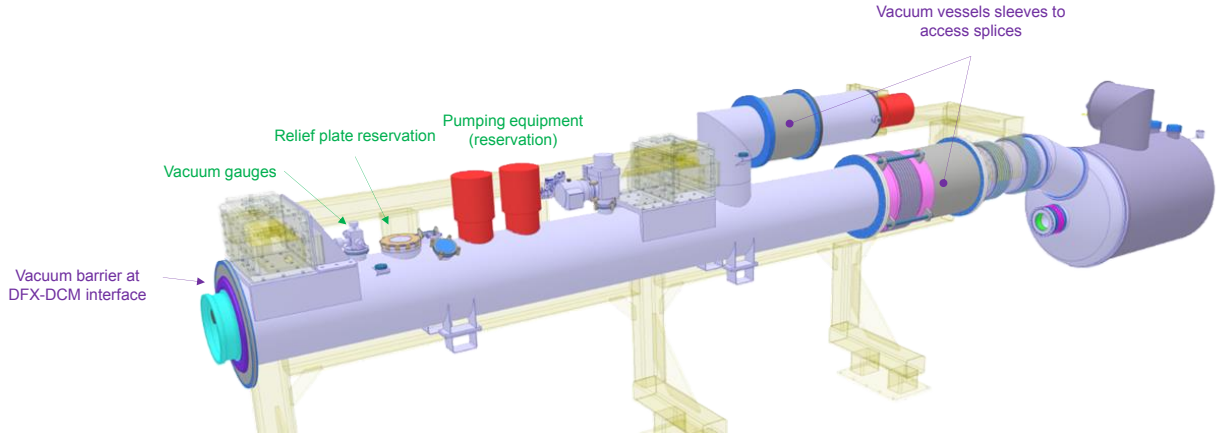

Figure 3-12: Engineering design of the D1-DFX connection module

3.7 Recombination dipole D2

Function, operational modes and powering: The recombination dipole is ramped with the energy of the LHC and is constant during squeeze. The two D2 apertures are in series. In D2, the fields point in the same direction in both apertures; this makes field quality control much more challenging than in the LHC dipoles, where the fields point in opposite directions.

The recombination dipole short model and prototype have been developed by INFN (Genova, IT), which also provides the series magnets in the framework of a collaboration agreement.

Conductor: The 15-mm-wide Nb-Ti cable used for the outer layer of the main LHC dipole is adopted. The required unit length about 2/3 of the LHC main dipole's outer layer unit length (780 m).

Coil, current density and margin: We selected a conservative margin, operating at 68% of the load line with a 15-mm-width coil, and an operational field of 4.5 T. In these conditions, the approach used in the present D2 design, that is using iron to magnetically decouple the two apertures, leads to large saturation effects. An alternative approach using left–right asymmetric coils was therefore adopted [33] to compensate for the cross-talk between the two apertures (see Figure 3-13). A very careful optimization is needed to find the best solution. After several iterations, a cross-section was found where the left–right asymmetry is only given by the angles of the blocks, but the number of cables per block is the same [34]. This allows for much simpler coil heads.

Lengths and transverse size: The magnetic length is 7.78 m. The magnet requires an adequate iron thickness to reduce the fringe field. An elliptical iron yoke is proposed, of 570 mm vertically and 630 mm horizontally.

Mechanical structure: The accumulation of Lorentz forces corresponds to a pressure in the midplane of about 40 MPa. A self-supporting stainless-steel collar, one per aperture, is considered. The two apertures are then inserted in an Al skin providing the relative alignment. The whole pack is inserted in the iron. Peak stress during collaring is of the order of 100 MPa [35].

Protection: Protection will be based on quench heaters using the standard LHC dipole technology (used also in D1). Hotspot temperature is estimated to be below 250 K.

Field quality: This is the main issue for this magnet: the square design of the central aperture in the iron and its elliptical shape is imposed by field quality optimization, namely the reduction of the field harmonics due to saturation. Cross-talk is optimized via the asymmetric cross-section, and the saturation through an iron shaping. In absence of iron and for a collared coil in stand-alone mode, quadrupole and sextupole components are of

the order of 200 units. The compensation due to the presence of the other coil and of the iron shaping allows to reduce these components within few units, i.e. has to work with a precision of the order of 1%.

Cooling: The magnet is in a static bath of pressurized HeII. Direct cooling is ensured via a cold finger.

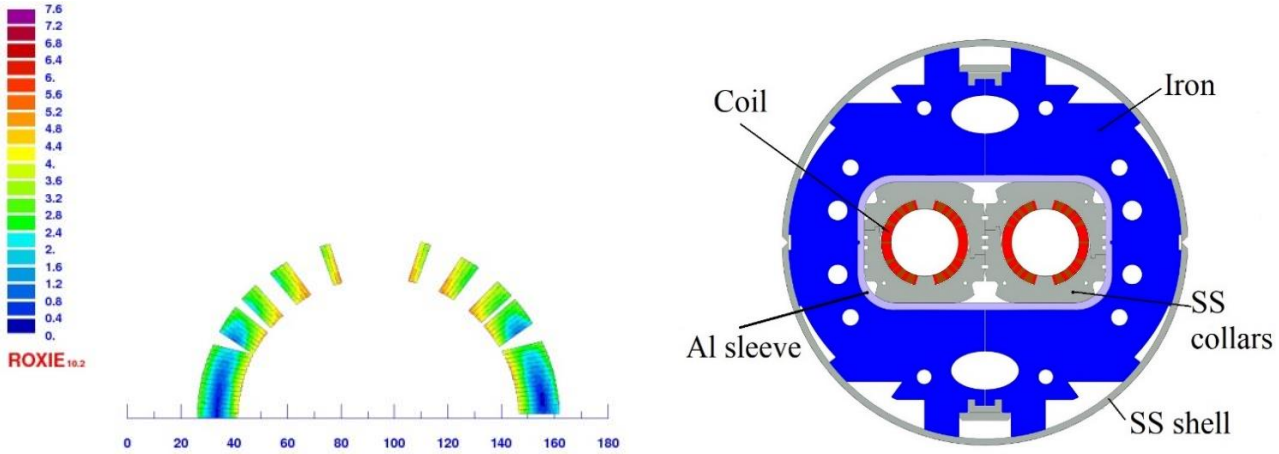

Figure 3-13: Sketch of recombination dipole cross-section. Asymmetric coil (left) and magnet cross-section (right). Note the elliptical shape of the yoke.

Cryostat: The cryostat has the same geometry as the triplet cryostat (see Figure 3-5).

3.8 D2 correctors

Function, operational modes and powering: D2 orbit correctors have to be installed for each beam and each plane (horizontal and vertical), with an integrated strength of 5 T·m, and an aperture of 105 mm. These correctors are used to control the crossing angle and to correct the closed orbit, and therefore they should be powered in a wide range of configurations. The large electromagnetic coupling and the stringent field quality requirement (all harmonics within 10 units for all combinations of currents) limit the main field to 2.60 T; this gives a magnetic length is 1.92 m. Horizontal and vertical correctors share the same longitudinal position for beam 1 and 2 respectively, and are followed by a vertical (beam1) and horizontal (beam2) corrector. In this configuration the magnetic cross-talk is less severe than in a case with horizontal-horizontal (or vertical/vertical) correctors in both beams (see Figure 3-14). These requirements make the D2 corrector as the ideal test bed for the canted cos-theta design, which provides the advantage of low operational current, and simple components and assembly procedures [36]. It will be the first time that a magnet based on this design will be used in a high energy physics accelerator.

The D2 corrector prototypes have been developed in CERN and shall be provided as in-kind contribution by a by IHEP (Beijing, CN), with the support of other Institutes.

Conductor: a 0.825 mm diameter Nb-Ti strand with characteristics similar to the LHC shall be used. Strand will be manufactured in China.

Coil, current density, and margin: Ten strands are wound in the groove, with 365 turns per magnet. The inclination of the winding of the top of the groove is 30º with respect to beam axis. The nominal bore field is 2.60 T, the peak field is 2.94 T, the operational current is ~400 A with a loadline fraction ~50%. Ten wires are wound in the same groove; the former+wire is then impregnated with CTD-101K®.

Lengths and transverse size: The magnet has a mechanical length of 2.2 m. The diameter is the same of the D2 cold mass, i.e. 614 mm.

Mechanical structure: In this design, the former is providing the position of the cable and the mechanical support. Each layer (in the two opposite direction of the angle, see Figure 3-14) is a 10 mm thick tube with a 5.2 mm deep and 1.1 mm width groove to house the ten strands. The two tubes contacting the two windings are surrounded by a third 10-mm-thick tube to limit the deformations due to Lorentz forces within 0.1 mm.

Protection: The low-current / large inductance of this type of design requires the use of a dump resistor. The resistance is set at 1.4 Ω, allowing to keep the voltages well below 1000 V. Even with this large value of resistance, energy extraction and quench propagation are not enough to keep the hotspot temperature below a safe value of 250 K. The magnet protection has to rely on the quench back induced in the former by the initial *dI/dt* given by the energy extraction. This mechanism is very effective and has been verified on short models and prototypes.

Field quality: The challenge in these magnets is the cross-talk between the apertures. Since for D2 the beam distance is 188 mm, and the aperture is 105 mm, little space is left for the iron to decouple the two apertures [37]. No optimization can be made through the coil cross-section as is the case in D2 since these magnets have to be powered with any combination of currents. The solution is to keep a thin coil, and to maximize the iron thickness. Requirements on field quality are to have all multipoles below 10 units.

Cooling: The magnets will share cooling with D2, so will have heat exchangers in the same position.

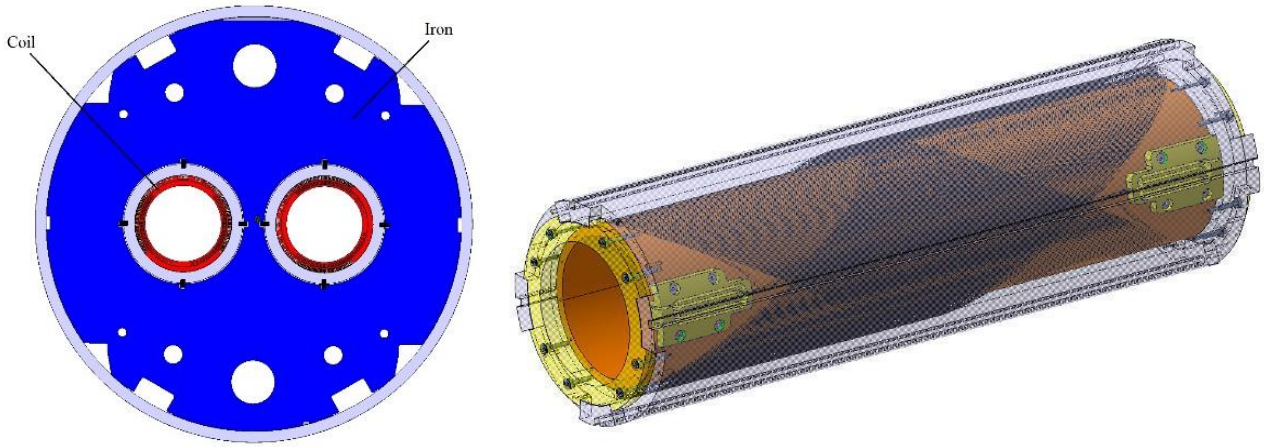

Figure 3-14: Cross-section of D2 orbit corrector (left) and 3D view of the short model coil (right).

3.9 Q4, Q5 and Q6

Both Q4 and Q5 will be moved from their positions in the LHC layout by about 10 m in the opposite direction of the interaction point to adapt to the new optics of the HL-LHC; they will work in the same operational conditions as in the LHC. In the first version of the project, a larger Q4 of 90 mm aperture was planned (MQYY) whose cross-section is shown in Figure 3-15. A short model magnet has been built in collaboration with CEA (Saclay-France); moreover, two full length prototypes are in construction in the industry with a European initiative (EC-H2020-QUACO). The Q6 magnet will not be modified and will be operated at 4.5 K as it is today in the LHC.

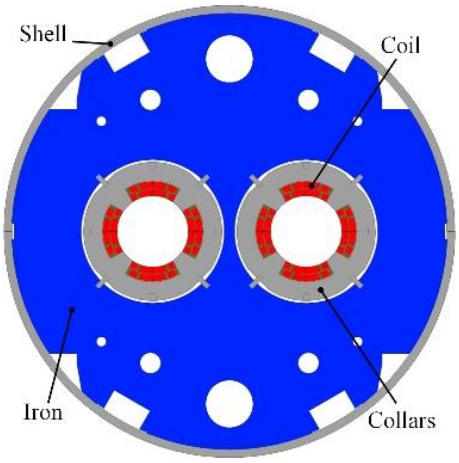

Figure 3-15: MQYY 90 mm aperture cross-section. This magnet is not anymore in the HL-LHC baseline.

3.10 Other modifications for the upgrade: sextupole (MS) in Q10 and magnets in IR3-IR7

The four cold masses of Q10 around IP1 and IP5 require a modification to include a lattice sextupole (MS) corrector. In the first version of the project, the two Q5 in IR6 were replaced by a new cold mass with two MQY each. In a second iteration the present LHC Q5 was kept for the HL-LHC, but the operational temperature was lowered from 4.5 K to 1.9 K to allow a larger strength. Further optimizations of the optics allowed to also avoid this modification, and in the present baseline the Q5 in IR6 has no modifications.

A Few of the MBW and MQW in IR3 and IR7 will have in the HL LHC era a radiation dose above the safe limit [40]. Consolidation actions have been taken to make these magnets able to survive the expected integrated luminosity of the HL-LHC; therefore, the initial plan of manufacturing radiation-hard MBW and MQW has been abandoned.

3.11 Magnets test plan

In general, magnets will be tested individually in a vertical test station, and then horizontally in the final cold mass assembly within the final cryostat, with the exception of Q2 and D2 whose length does not allow vertical testing. Many power tests will be done in laboratories collaborating with CERN (BNL for vertical test of Q1/Q3, FNAL for horizontal test of Q1/Q3, KEK for vertical test of D1, LASA for vertical test of high order correctors, IMP (Lanzhou-China) for vertical test of D2 correctors, FREIA (Univ. of Uppsala, Sweden) for vertical test of MCBXFB. For the D2 correctors and for the high order correctors, performance shall be assessed in LASA and IMP at 4.5 K.

All test will require reaching the so-called ultimate current, corresponding to operation in the HL-LHC at 7.5 TeV. All main magnets will undergo a thermal cycle to verify the training. A string including the magnets from Q1 to D1 will be assembled in the CERN test facility (SM18) and tested prior to the installation of the HL-LHC components in the LHC tunnel (See Chapter 16).

3.12 References

[1] O. Bruning, L. Rossi, Eds. “The High Luminosity Large Hadron Collider”, Advances Series on Directions in High Energy Physics **24,** (World Scientific, Singapore 2015), DOI: 10.1142/9581.

[2] E. Todesco *et al.*, A first baseline for the magnets in the high luminosity LHC insertion regions, *IEEE Trans. Appl. Supercond.* **24** (2014) 4003305, DOI: 10.1109/TASC.2013.2288603.

[3] G. Sabbi, Nb_3Sn IR Quadrupoles for the High Luminosity LHC, *IEEE Trans. Appl. Supercond.* **23**, 2013, DOI: 10.1109/TASC.2003.812635.

[4] L. Rossi and E. Todesco, Electromagnetic design of superconducting quadrupoles, *Phys. Rev. Spec. Top. Accel. Beams* **9** *(2006)* 102401, CERN-AT-2006-016-MCS.

[5] A. Tollestrup *et al.*, The development of superconducting magnets for use in particle accelerators: from Tevatron to the LHC, *Rev. Accel. Sci. Technol.* **1** (2008) 185-210, DOI: 10.1142/S1793626808000101.

[6] P. Ferracin *et al.*, Limits to high field magnets for particle accelerators, *IEEE Trans. Appl. Supercond.* **22** (2012) 4003106, DOI: 10.1109/TASC.2011.2181143.

[7] P. Ferracin *et al.*, Magnet design of the 150 mm aperture low-beta quadrupoles for the high luminosity LHC, *IEEE Trans. Appl. Supercond.* **24** (2014), DOI: 10.1109/TASC.2013.2284970.

[8] Q. Xu *et al.*, Design optimization of the new D1 dipole for HL-LHC upgrade, *IEEE Trans. Appl. Supercond.* **24** (2014) 4000104, DOI: 10.1109/TASC.2013.2280812.

[9] G. Apollinari, I. Bejar Alonso, O. Brüning, M. Lamont, L. Rossi, eds., High Luminosity Large Hadron Collider (HL-LHC): Preliminary Design Report. CERN-2015-005, DOI: 10.5170/CERN-2015-005

[10] HL-LHC ECR WP3. Baseline for the Inner Triplet Main Circuit, EDMS: 1832082 and HL-LHC ECR WP7, energy extraction systems for HL-LHC RCBX circuits, EDMS: 2360296.

[11] S. Caspi *et al.*, Test results of LARP Nb_3Sn quadrupole magnets using a shell-based support structure (TQS), *IEEE Trans. Appl. Supercond.* **19** (2009) 1221–1225, DOI: 10.5170/CERN-2009-001.117.

[12] G. Ambrosio *et al.*, Test results of the First 3.7 m long Nb_3Sn quadrupole by LARP and future plans, *IEEE Appl. Supercond.* **21** (2011) 1858–1862, DOI: 10.1109/TASC.2010.2089586.

[13] H. Felice *et al.*, Design of HQ – A high field, large bore Nb_3Sn Quadrupole Magnet for LARP, *IEEE Trans. Appl. Supercond.* **19** (2009) 1235–1239, DOI: 10.1109/TASC.2009.2019105.

[14] E. Todesco, Quench limits in the next generation of magnets, CERN Yellow Report 2013-006, 2013, DOI: 10.5170/CERN-2013-006.10.

[15] T. Salmi *et al.*, Modeling heat transfer from quench protection heaters to superconducting cables in Nb_3Sn magnets, *CERN Yellow Report* **2013-006** (2013) p. 30–37, DOI: 10.5170/CERN-2013-006.30.

[16] V. Marinozzi *et al.*, Study of quench protection for the low β quadrupole for the LHC luminosity upgrade. *IEEE Trans. Appl. Supercond*. **25** (2015) 4002905, DOI: 10.1109/TASC.2014.2383435.

[17] E. Ravaioli *et al.*, New coupling loss induced quench protection system for superconducting accelerator magnets, *IEEE Trans. Appl. Supercond.* **24** (2014) 0500905, DOI: 10.1109/TASC.2013.2281223.

[18] S. Izquierdo Bermudez *et al.*, Coil end optimization of the low β quadrupole for the high luminosity LHC, Applied Superconductivity Conference 2014, IEEE Trans. Appl. Supercond. 25 (2015), CERN-ACC-2015-0023.

[19] R. Gupta, Tuning shims for high field quality in superconducting magnets, *IEEE Trans. Magn.* **32** (1996) 2069–2073, DOI: 10.1109/20.508569.

[20] P. Hagen, Study of magnetic shimming in triplet magnets, Milestone Report 36 of HiLumi project.

[21] R. Van Weelderen, Superfluid helium cooling, Milestone Report 42 of HiLumi project.

[22] D. Duarte Ramos *et al.*, talk given at WP3 meeting on 28 January 2014.WP3 Web page.

[23] J. Garcia Matos *et al.*, talk given at WP3 meeting on 17 July 2014. WP3 Web page.

[24] M. Karppinen, Corrector magnets for the LHC upgrade phase-1, CERN EDMS 1039976, and R. Ostojic *et al.*, Conceptual design of the LHC interaction region upgrade: Phase I, LHC Project Report **1163** (2008) p. 42.

[25] F. Toral *et al.*, Development of radiation resistant superconducting corrector magnets for the LHC upgrade, *IEEE Trans. Appl. Supercond.* **23** (2013), DOI: 10.1109/TASC.2013.2239698.

[26] G. Volpini *et al.*, Nb-Ti superferric corrector magnets for the LHC luminosity upgrade, *IEEE Trans. Appl. Supercond.* **25** (2015), DOI: 10.1109/TASC.2014.2378377.

[27] T. Nakamoto *et al.*, Model magnet development of D1 beam separation dipole for the HL-LHC upgrade, *IEEE Trans. Appl. Supercond.* **25** (2015) 4000505, DOI: 10.1109/TASC.2014.2361404.

[28] T. Nakamoto *et al.*, Construction of superconducting magnet system for the j-PARC neutrino beam line, *IEEE Trans. Appl. Supercond.* **20** (2010) 208–213, DOI: 10.1109/TASC.2009.2038800.

[29] M. Anerella *et al.*, The RHIC magnet system, *Nucl. Instrum. Meths. A* **499** (2003) 280–315, DOI: 10.1016/S0168-9002(02)01940-X.

[30] Y. Ajima *et al.*, The MQXA quadrupoles for the LHC low-beta insertions, *Nucl. Instrum. Meths. A* **550** (2005) 499–513, DOI: 10.1016/j.nima.2005.04.092.

[31] B. Bellesia, J. P. Koutchouk and E. Todesco, Field quality in low-beta superconducting quadrupoles and impact on the beam dynamics for the Large Hadron Collider, *Phys. Rev. STAB* **10**, 2007, DOI: 10.1103/PhysRevSTAB.10.062401.

[32] B. Bellesia, C. Santoni and E. Todesco, Random errors in superconducting dipoles, 10th European Particle Accelerator Conf. (2006) 2601–2603, CERN-AT-2006-010-MAS.

[33] V. Kashikhin, *et al.*, Design study of 2-in-1 large aperture IR dipole (D2) for the LHC luminosity upgrade Particle Accelerator Conference (2007) 464-6, and G. Sabbi *et al.*, Conceptual Design Study of the High Luminosity LHC Recombination Dipole, 5th International Particle Accelerator Conf., (2014) 2712-4, DOI: 10.1109/PAC.2007.4440246.

[34] P. Fabbricatore *et al.*, talk given at WP3 meeting on 17 September 2014.

[35] S. Farinon *et al.*, talk given at WP3 meeting on 17 September 2014, WP3 Web page.

[36] G. Kirby, J. Rysti, *et al.*, Hi-Lumi LHC Twin-Aperture Orbit Correctors Magnet System Optimisation, *IEEE Trans. Appl. Supercond.* **27** (2017), DOI: 10.1109/TASC.2016.2633424.

[37] J. Rysti *et al.*, talk given at WP3 meeting on 17 September 2014.

[38] G. Kirby *et al.*, Performance of the 1-m model of the 70 mm twin aperture superconducting quadrupole for the LHC insertions, *IEEE Trans. Appl. Supercond.* **11** (2001) 1641.P. P. Granieri *et al.*, Thermally enhanced cable insulation for the Nb-Ti high luminosity LHC inner triplet model, *IEEE Trans. Appl. Supercond.* **22** (2012) DOI: 10.1109/77.920095 and DOI: 10.1109/TASC.2012.2183669.

[39] M. Segreti *et al.*, A Nb-Ti 90 mm double aperture quadrupole for the high luminosity LHC upgrade, *IEEE Trans. Appl. Supercond.* **25** (2015) 4001905, DOI: 10.1109/TASC.2014.2366517.

[40] N. Mariani, P. Fessia, et al., talk given at WP3 meeting on 31 August 2016, WP3 Web page.

[41] HL-LHC ECR - WP12 - Shielded Beam Screens Operating Temperature for the Triplets (Q1,Q2,Q3), correctors package and D1, EDMS: 2112891.

[42] HL-LHC ECR WP15-WP3: Alignment of the D1 separation dipole in IR1 and 5 to maximize available beam aperture, EDMS: 2374033.

[43] HL-LHC ECR - WP15.4 Remote Alignment, EDMS: 1823448.

[44] HL-LHC ECR - WP3 Change Of Quadrupole, Sextupole, Octupole And Decapole Correctors Integrated Field, EDMS: 1963788.

[45] HL-LHC ECR - WP3. Need of a connection module LDQD (D1-DFX), EDMS: 2210558.

[46] HL-LHC ECR - WP3. Change of operational temperature in Q5 IR6 from 1.9 K to 4.5K, EDMS: 2117079.

[47] HL-LHC Decision management: WP3 - fine tuning of b6, EDMS: 2019517.

[48] HL-LHC ECR - WP3. Change of Baseline for HL-LHC Warm magnets, EDMS: 1832073.

[49] HL-LHC ECR - WP3 Increase of iron yoke holes diameter from 60 to 61 mm for heat exchangers in D1 and MCQSXF, EDMS: 1865591.

[50] US HL-LHC AUP - MQXFA Final Design Report [US-HiLumi-doc-948], EDMS: 2031097.